2010

Structure–property relations of cyclic damage in a wrought magnesium alloy

J. D. Bernard
Mississippi State University

J. B. Jordon
Mississippi State University

M. F. Horstemeyer
Mississippi State University

H. El Kadiri
Mississippi State University

J. Baird
Mississippi State University, jkevinbaird@yahoo.com

See next page for additional authors

Available online at www.sciencedirect.com
ScienceDirect
Scripta Materialia 63 (2010) 751–756
Scripta MATERIALIA
www.elsevier.com/locate/scriptamat

Viewpoint Paper

Structure–property relations of cyclic damage in a wrought magnesium alloy

J.D. Bernard,[a] J.B. Jordon,[a,*] M.F. Horstemeyer,[a] H. El Kadiri,[a] J. Baird,[a] David Lamb[b] and Alan A. Luo[c]

[a] *Mississippi State University, Center for Advanced Vehicular Systems, 200 Research Blvd, Starkville, MS 39759, USA*
[b] *US Army RDECOM-TARDEC, Bldg. 215, (RDTA-S) Mail Stop 157, 6501 E. 11 Mile Road, Warren, MI 48397-5000, USA*
[c] *Chemical Sciences and Materials Systems Lab, General Motors Research & Development Center, MC: 480-106-224, 30500 Mound Road, Warren, MI 48090-9055, USA*

Available online 9 June 2010

Abstract—The fatigue properties of an extruded Mg–3Al–0Mn magnesium alloy component were evaluated experimentally. Fully reversed, strain control fatigue tests were conducted on specimens extracted from regions with a varying grain size and texture. Scanning electron microscopy was employed to establish structure–property relations between microstructure and cyclic damage. Relations were drawn between microstructural features such as particle size, grain size, initial Taylor factor and the number of cycles to failure.

Keywords: Structure–property; Fatigue; Magnesium alloys; Scanning electron microscopy

1. Introduction

Suresh's seminal work [1] discussed the history and nuances of small crack growth, and the issue of microstructural features playing a large role in the driving force and material resistance under cyclic loads. For aluminum alloys, Couper et al. [2] showed experimental data on how crack opening displacements change when a crack meets a particle, which was subsequently corroborated by micromechanical finite-element simulations [3,4]. As a result of these studies, along with other structure–property quantifications for aluminum alloys [5–8], McDowell et al. [9] developed a microstructure-sensitive multistage fatigue model that captured the general driving force-material resistance issues dependent on the pore, particle and grain size statistics.

Similar work has not been as advanced for magnesium alloys, although some work has been completed on quantifying the structure–property relationships under fatigue loads. For example, Horstemeyer and coworkers [10–13] examined microstructurally small crack growth rates for different magnesium alloys, and the effect of associated various microstructural features under high-cycle fatigue conditions. For low-cycle fatigue, Gall et al. [14–16] examined a cast AM60B magnesium alloy in situ with a scanning electron microscope under different environmental effects to study the microstructurally small crack growth rates. However, microstructure-sensitive multistage fatigue modeling is still in its infancy. In addition, for both the aluminum and magnesium alloys, the processing methods have focused on castings. It is envisioned that the next-generation magnesium alloys will use extruded and rolled products, and developing a more detailed understanding of their fatigue behavior is therefore warranted.

General Motors Research and Development Center (GM R&D) recently created a new extruded magnesium alloy, designated AM30 [17]. The low-cycle fatigue performance of this alloy was quantified, including the cyclic hardening and asymmetric behavior [18–20]. In terms of microstructural influences on fatigue damage, research has previously been conducted on similar magnesium alloys with regards to microstructural effects on the strain rate sensitivity [21] and grain size refinement effects on fatigue properties [22,23]. Magnesium alloys with a finer grain size exhibited a reduction in crack growth rate when compared to the same alloy with larger grains. Material orientation with respect to the extrusion direction and manganese content on fatigue life were shown to have a

* Corresponding author. Tel.: +1 662 325 8977; fax: +1 662 325 5433; e-mail: bjordon@cavs.msstate.edu

1359-6462/$ - see front matter © 2010 Acta Materialia Inc. Published by Elsevier Ltd. All rights reserved.
doi:10.1016/j.scriptamat.2010.05.048

Table 1. AM30 chemical composition (wt.%).

Al	Mn	Zn	Fe	Cu	Ni
3.4	0.33	0.16	0.0026	0.0008	0.0006

profound impact on both short and long crack development [24]. Furthermore, the authors suggested that the crack closure behavior was largely responsible for variations in the fatigue life of different specimen orientations. Further studies into the texture effects were conducted on a magnesium alloy, AZ31 [25]. These findings indicated that the fracture toughness of the material was significantly affected by the orientation of the specimen with respect to the extrusion direction.

The intent of this research is to further quantify the cyclic behavior of AM30 and to obtain relations between the microstructure of the material and cyclic damage. As such, structure–property relationships that correlate material texture, grain size and critical flaw size to fatigue life were determined.

2. Materials and experiments

Table 1 lists the chemical composition of the magnesium AM30 alloy employed in this study [17]. The specimens were machined from an extruded AM30 magnesium alloy crash rail parallel to the extrusion direction. These cylindrical dog-bone-shaped specimens had a gage length of 30 mm and a diameter of 6 mm. Since different regions of the rail exhibited varying average grain sizes and texture, multiple specimens were machined from six predetermined sections (shown later).

In order to reduce man-made surface-influenced fatigue cracks, the shoulder and gage section of each specimen were hand-ground in the longitudinal direction until the surface was free of all circumferential machining marks. The specimens were then degreased using ethanol. Fully reversed fatigue tests were conducted under constant total strain amplitude of 0.003 mm mm^{-1} at 3 Hz in ambient temperature and humidity. In order to properly control the strain amplitude, an extensometer was employed in the gage region of each specimen for up to 20,000 cycles. If the specimen did not fail by 20,000 cycles, the tests were stopped and switched to load-control, and testing was resumed at 20 Hz [18] until failure. Upon failure, the fracture surfaces were cut from the specimen and mounted for scanning electron microscopy (SEM) observation in a typical manner. In order to obtain high-resolution images and to prevent further oxidation, the specimens were sputter coated with gold–palladium for a period of 15 s prior to SEM imaging. After fatigue crack initiation particles were identified on each fracture surface, energy-dispersive X-ray analysis was conducted to determine the composition of the particles.

3. Results and discussion

Due to the high speed of the extrusion (2.7 m min^{-1}), limited recrystallization occurred in the matrix. Thus the extrusion deformation resulted in a strong texture. This texture promoted a marked aspect ratio of the particles with a preferential orientation in the matrix. As such,

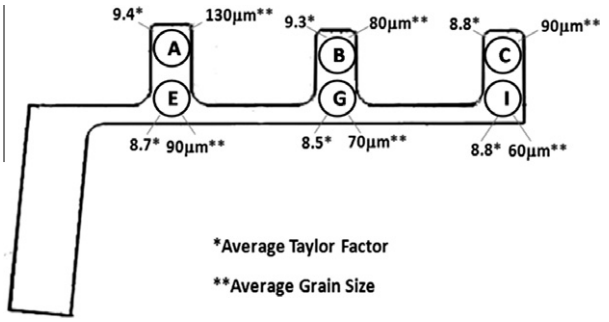

Figure. 1. The initial average grain size and initial Taylor factor in the extruded magnesium AM30 alloy. The fatigue specimens were machined from sections A, B, C, E, G, and I as indicated in the cross-sectional view of the extruded alloy.

the average initial grain size and initial Taylor factors based on electron backscatter diffraction (EBSD) results of the rail cross-section are shown in Figure. 1. Figure. 2 shows the specific EBSD results from section A. The initial Taylor factors were only used to provide a comparative analysis of the distribution of the material strength in the rail component. The calculated Taylor factors do not reflect the actual strength of the material. The average Taylor factors were calculated based on combined basal $\langle a$, prismatic $\langle a\rangle$, pyramidal $\langle c+a\rangle$ and $\{10\bar{1}2\}\langle 10\bar{1}\bar{1}\rangle$ tensile twin modes. The critically resolved shear stresses (CRSSs) used in these calculations corresponded to the CRSS ratios calculated by Jain et al. [26] for an AZ31 alloy. The fatigue specimens tested in this study were taken from the six regions (A, B, C, E, G, and I), as indicated in Figure. 1. The number of cycles to failure for the given strain amplitude for each region is displayed in Table 2.

Post-mortem fractography was conducted on all of the fatigue specimens. Each of the fracture surfaces was examined by SEM in order to determine the sources of crack initiation. The fracture surfaces of the magnesium

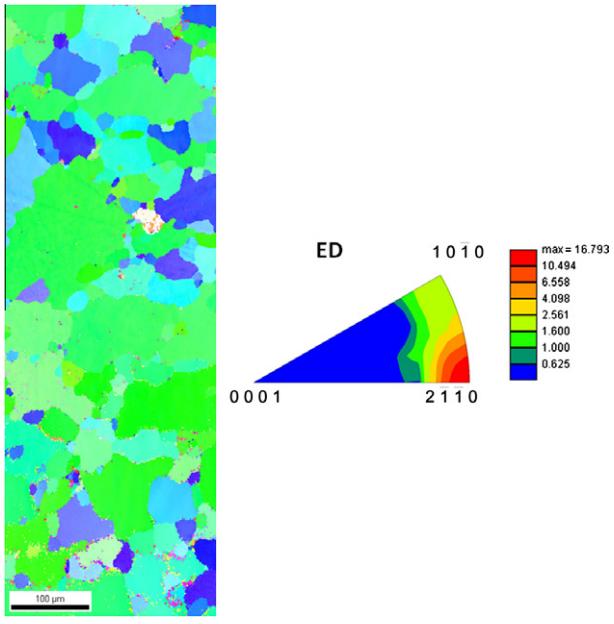

Figure. 2. EBSD mapping showing the texture characteristics of section A in the extruded direction (ED).

Table 2. Summary of cycles to failure from various regions of the extruded magnesium AM30 alloy.

Section	Cycles to failure	Average Taylor factor	Average grain size (μm)
A	8480	9.4	130
A	16295	9.4	130
A	22258	9.4	130
B	8735	9.3	80
B	15546	9.3	80
B	18530	9.3	80
C	17358	8.8	90
E	33096	8.7	90
E	168063	8.7	90
E	230121	8.7	90
G	24165	8.5	70
G	41592	8.5	70
G	80204	8.5	70
I	64671	8.8	60
I	251273	8.8	60

AM30 alloy displayed classic indications of fatigue damage. Typical river marks flowing outward from a single location at the surface were observed on all specimens. Figure. 3a shows an overview image of the fracture surface. The crack initiation site, indicated at the bottom of Figure. 3a, is shown in Figure. 3b. Figure. 3c shows a higher magnification of the particle which initiated the crack. Of the 15 fracture surfaces examined, intermetallic particles were found to be the source of crack initiation on eight of the specimens tested. On the specimens where particles were not found, signs of oxidation were present at some of the crack initiation sites. As such, the oxidation prevented observation of the source of the crack initiation. In addition, a few specimens contained no particles, and no oxidation was found at the intiation site. This suggests that crack initiation could have occurred due to a persistent slip band (PSB) [14–16] or a twinning–detwinning phenomenon [27]. The intermetallics were identified through chemical analysis as Al–Mn binary (Al8–Mn5) particles. As such, these types of particles appear to be more brittle than the surrounding matrix and tended to fracture rather than debond. Fracturing of the intermetallic particles was observed on all of the surfaces imaged via SEM, and no evidence of debonding was observed. Furthermore, all of the particles were found to be located on the surface of the specimen, and no subsurface particles initiated a fatigue crack. Each of the cyclic failures stemmed from only one particle and not multiple particles.

The typical initiation sites revealed early striations starting at the particle–matrix interface. While not conducted in this study, crack growth rates can be estimated from striation spacing for the microstructrually small crack regime. Furthermore, twins and slip bands were observed not to align with the direction of crack propagation. This is probably due to the effect of crystal orientation, where the crack propagated through the path of least resistance through the slip planes. While the crack propagation path is generally radially outward at the macroscale, the crack may have propagated in directions that corresponded to the active slip or twin systems ahead of the crack tip.

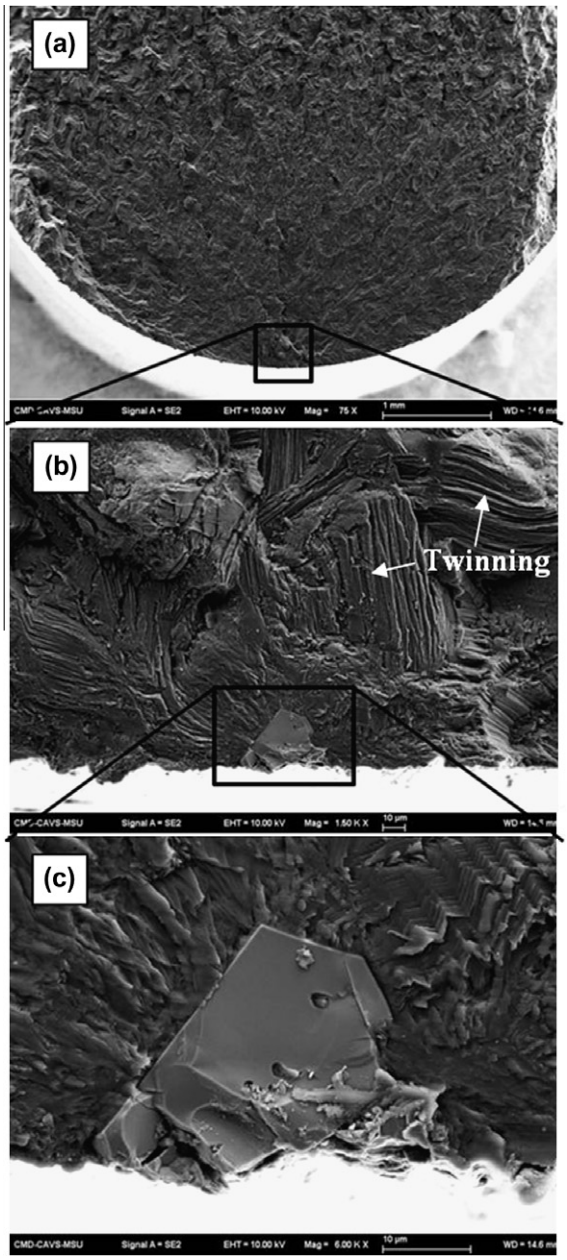

Figure. 3. Post-mortem fractographs of magnesium AM30 alloy. This particular specimen was taken from region E and failed after 33,096 cycles. (a) Typical overview of the fracture surface which highlights the profuse glide twinning responsible for the crack propagation. (b) The fatigue crack initiated from an intermetallic particle as indicated in the bottom of (a). Also highlighted is the substantial extent of glide twinning in nearly all of the grains that were subject to crack propagation. The regions near the intermetallic show smaller twins, indicating that twinning played a role in promoting crack nucleation at the particle. (c) A high magnification of the particle as indicated in (b).

Also observed in the SEM images was evidence of twinning on the fatigue fracture surfaces similar to that was reported in the literature [18,19]. The mechanisms of twinning and detwinning have the potential to create nucleation sites of a substantial number of small cracks that feed ahead of the main propagating crack. These potential sites could correspond to alignments of twinning dislocations left behind by the successive alternations of twinning and detwinning [28,29]. The slip bands observed

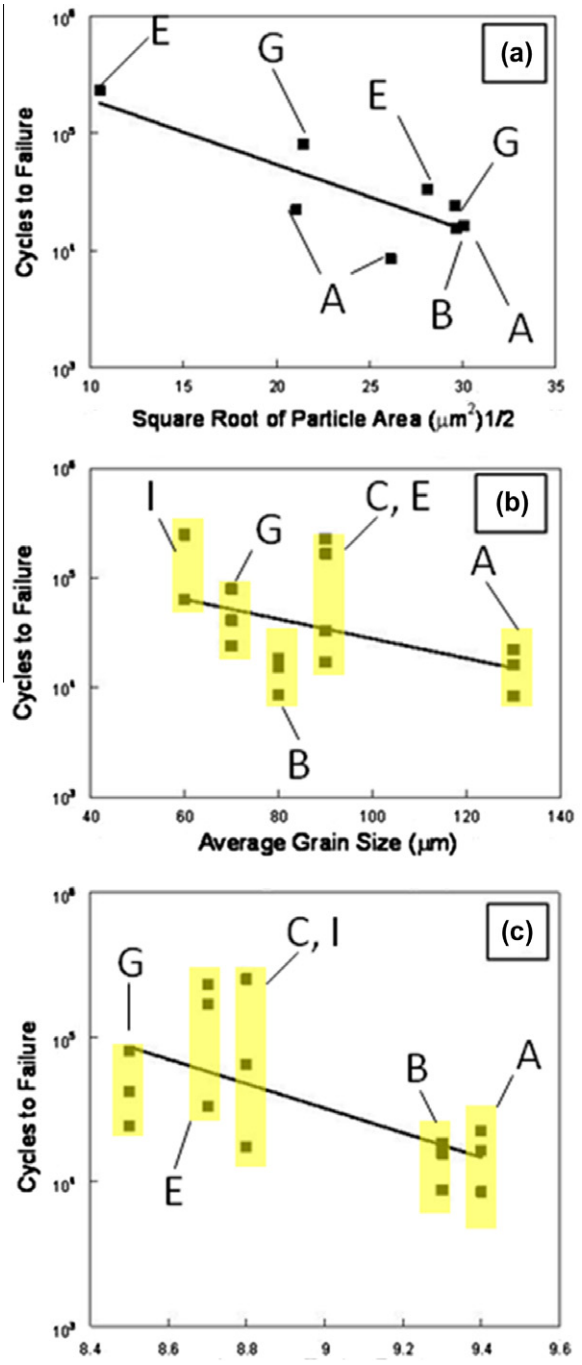

Figure. 4. Number of cycles to failure vs. the square root of the particle area (a), average grain size (b), and average Taylor factor (c) for the magnesium AM30 alloy. The locations from the rail cross-section of the specimens are also shown.

close to the particle responsible for nucleation may correspond to basal slip activity necessary to accommodate plasticity at a low stress level. As the crack propagates, the stress rapidly attains a level to consistently initiate twinning. Consistent twinning ahead of the crack tip could be explained by the nature of stress triaxiality ahead of the crack tip that would always find an adequate Schmid factor exceeding the CRSS of twinning, regardless of the grain orientation.

The contribution of twinning mechanisms to crack propagation is beyond the scope of this paper and is the subject of another publication. However, part of the objective of this study was to correlate structure–property relationships in order to predict the scatter that is typically observed in fatigue studies. The square root of the particle area vs. the number of cycles to failure is shown in Figure. 4a. The area of each particle was calculated using an image analyzing software program [30]. The trend shows that specimens with smaller particles had greater fatigue resistance, and therefore better fatigue life, when compared to specimens with larger particles.

To further characterize the microstructure of the AM30 alloy in regards to the fatigue behavior, the average grain size and initial Taylor factors are plotted against the number of cycles to failure. Again, the specimens were machined from sections that contained various grain sizes and calculated initial Taylor factors. Figure. 4b displays the number of cycles vs. average grain size. While this plot displays significant scatter, the trend suggests that the alloy exhibits greater fatigue resistance for smaller grains compared to specimens with larger grains. This observation is somewhat unexpected considering larger grains typically provide better fatigue resistance in steel and aluminum alloys by providing grain boundrary blocking that slows the rate of crack propagation. However, in this present study, smaller grains provided better fatigue resistance, which is consistent with a similar extruded Mg alloy [22].

Likewise, Figure. 4c shows that the smaller Taylor factor values resulted in generally higher fatigue lives. While the plot in Figure. 4c also displays some level of scatter, the trend suggests that the alloy exhibits greater fatigue resistance for smaller initial Taylor factors compared to specimens with larger Taylor factors. The calculation of the Taylor factors was derived from the summation of the amount of shear of the active slip systems and then normalized by the deformation step [27]. Thus, higher initial Taylor factors mean more local shear compared to lower Taylor factors. Since crack initiation is dependent on local shear strain, higher Taylor factor values imply that crack initiation will occur earlier compared to lower Taylor factors. However, to confirm this notion, future fatigue work will be conducted.

4. Conclusions and perspectives

Based on the results of this fatigue study of an extruded magnesium alloy, the following conclusions are given:

1. The fatigue crack initiation was dominated by intermetallic particles consisting of Mg–Al–Mn located at the surface. In general, the specimens that exhibited higher fatigue resistance typically had fatigue cracks that initiated from smaller intermetallics. Likewise, larger particles that initiated the fatigue cracks had lower cycles to failure.
2. Mg–Al–Mn particles that initiated the fatigue cracks were observed to fracture rather than debond.
3. Greater fatigue life was generally associated with specimens that contained smaller grain sizes. The larger the average grain size, the lower the fatigue life. In contrast, the smaller the grain size, the higher the fatigue life.

4. In general, specimens with a lower average initial Taylor factor exhibited a better fatigue resistance compared to specimens with a higher calculated Taylor factor.

The extrusion example presented in this paper illustrates that the structure–property relations are just scratching the surface of what needs to be studied when trying to achieve greater understanding of magnesium alloys. Clearly, some work on the mechanical fatigue of cast magnesium alloys has had more progress than the work on extruded parts. However, for magnesium to compete with steel and aluminum alloys for use in mechanical and structural components, several issues need to be addressed. Some of these ideas are provided in the following:

1. Frequently in examining fracture surfaces of magnesium failed specimens, oxide layers are found to exist on top of the magnesium. The question remains: does the oxide form during the fatigue loading as new free surface arises from the fatigue process, or do the oxides exist prior to the cyclic loading arising from the materials processing? If the oxide forms during the fatigue process, does it act to resist the fatigue crack growth or enhance it?
2. Since the electrochemical potential of magnesium is so high, the corrosive rate will, in general, be greater than that of steel or aluminum. As such, quantifying the coupled chemomechanical effects of magnesium under stress-corrosion cracking has been elusive. Studies to quantify the surface corrosion rates coupled with the mechanical loading effects are certainly an outstanding issue when examining stress-corrosion cracking. However, hydrogen diffusion can also occur and induce internal cracking. Sorting out these different mechanisms will be key to any sort of a theoretically coupled chemomechanical fatigue model.
3. Although some preliminary studies were conducted to analyze the driving force-material resistance issues for magnesium alloys, as discussed earlier, more quantitative studies that delineate each different microstructural feature on the local crack growth rate are warranted. For example, more in situ studies employing SEM methods would be helpful to distinguish the local fatigue crack growth rates for cracks running into twins, particles, pores, dendrites and grains. Each of these different microstructural features represents a different length scale and, hence, provides a different resistance to the microstructurally small crack.
4. The low-cycle and high-cycle fatigue tests have typically not included the effects of overloads or changing load histories. In aluminum and steel alloys, the overloads induce various history effects, thus, giving certain fatigue trends. However, these alloys do not have a hexagonal close-packed crystal structure like magnesium. Some studies should examine the history effects of changing stress amplitudes, loading frequencies, temperature and environment, and should be performed to quantify the true material behavior for practical engineering use.
5. Clearly, without having the structure–property relations for fatigue of magnesium alloys, the material models would not have the robustness required to be predictive. Multiscale materials modeling needs to be performed to provide understanding of the cause–effect relations for microstructurally small cracks undergoing fatigue.

Acknowledgements

The authors would like to recognize Richard Osborne, James Quinn, Xuming Su, John Allison, Robert McCune, Don Penrod, and Matthew Castanier for their encouragement of this study. This material is based upon work supported by the Department of Energy and the National Energy Technology Laboratory under Award Number No. DE-FC26-02OR22910, and the US Army TACOM Life Cycle Command under Contract No. W56HZV-08-C-0236 through a subcontract with Mississippi State University, and was performed for the Simulation Based Reliability and Safety (SimBRS) research program. This report was prepared as an account of work sponsored by an agency of the United States Government. Neither the United States Government nor any agency thereof, nor any of their employees, makes any warranty, express or implied, or assumes any legal liability or responsibility for the accuracy, completeness, or usefulness of any information, apparatus, product, or process disclosed, or represents that its use would not infringe privately owned rights. Reference herein to any specific commercial product, process, or service by trade name, trademark, manufacturer, or otherwise does not necessarily constitute or imply its endorsement, recommendation, or favoring by the United States Government or any agency thereof. The views and opinions of authors expressed herein do not necessarily state or reflect those of the United States Government or any agency thereof. Such support does not constitute an endorsement by the Department of Energy of the work or the views expressed herein. UNCLASSIFIED: Dist A. Approved for public release.

References

[1] S. Suresh, Fatigue of Metals, Cambridge University Press, Cambridge, 1998.
[2] M.J. Couper, A.E. Neeson, J.R. Griffiths, Fatigue Fract. Engng. Mater Struct. 13 (1990) 213.
[3] J. Fan, D.L. McDowell, M.F. Horstemeyer, K.A. Gall, Engng. Fract. Mech. 68 (2001) 1687.
[4] J. Fan, D.L. McDowell, M.F. Horstemeyer, K.A. Gall, Engng. Fract. Mech. 70 (2003) 1281.
[5] K. Gall, N. Yang, M. Horstemeyer, D.L. McDowell, J. Fan, Met. Mater. Trans. A 30 (1999) 3079.
[6] K. Gall, N. Yang, M. Horstemeyer, D.L. McDowell, J. Fan, Fatigue Fract. Engng. Mater. Struct. 23 (2000) 159.
[7] K. Gall, M.F. Horstemeyer, D.L. McDowell, J. Fan, Mech. Mater. 32 (2000) 277.
[8] K. Gall, M.F. Horstemeyer, B.W. Degner, D.L. McDowell, J. Fan, Int. J. Fract. 108 (2001) 207.
[9] D.L. McDowell, K. Gall, M.F. Horstemeyer, J. fan, Engng. Fract. Mech. 70 (2003) 49.
[10] M.F. Horstemeyer, N. Yang, K.A. Gall, D.L. McDowell, J. Fan, P. Gullett, Fatigue Fract. Engng. Mater. Struct. 25 (2002) 1045.
[11] M.F. Horstemeyer, N. Yang, K.A. Gall, D.L. McDowell, J. Fan, P. Gullett, Acta Mater. 52 (2004) 1327.
[12] H. El Kadiri, Y. Xue, M.F. Horstemeyer, J.B. Jordon, P.T. Wang, Acta Mater. 54 (2006) 5061.

[13] H.E. Kadiri, M.F. Horstemeyer, J. Jordon, Y. Xue, Met. Mater. Trans. A 39 (2008) 190.
[14] K. Gall, G. Biallas, H.J. Maier, P. Gullett, M.F. Horstemeyer, D.L. McDowell, Met. Mater. Trans. A 35 (2004) 321.
[15] K. Gall, G. Biallas, Hans J. Maier, P. Gullett, M.F. Horstemeyer, D.L. McDowell, J. Fan, Int. J. Fatigue 26 (2004) 59.
[16] K. Gall, G. Biallas, H.J. Maier, M.F. Horstemeyer, D.L. McDowell, Mater. Sci. Engng. A (2004) 143.
[17] A.A. Luo, A.K. Sachdev, Met. Mater. Trans. A 38 (2007) 1184.
[18] S. Begum, D.L. Chen, S. Xu, Alan A. Luo, Met. Mater. Trans. A 39A (2008) 3014.
[19] C.L. Fan, D.L. Chen, A.A. Luo, Mater. Sci. Eng. A 519 (2009) 38.
[20] R. Zeng, E. Han, W. Ke, W. Dietzel, K.U. Kainer, A. Atrens, Int. J. Fatigue 32 (2010) 411.
[21] H. Kim, Y. Lee, C. Chung, Scr. Mater. 52 (2005) 473.
[22] F. Yang, S.M. Yin, S.X. Li, Z.F. Zhang, Mater. Sci. Eng. A 491 (2008) 131.
[23] Z.B. Sajuri, Y. Miyashita, Y. Hosokai, Y. Mutoh, Int. J. Mech. Sci. 48 (2006) 198.
[24] H. Somekawa, T. Mukai, Scr. Mater. 53 (2005) 541.
[25] D. Raabe, Acta Mater. 43 (1995) 1531.
[26] A. Jain, S.R. Agnew, Mater. Sci. Eng. A 462 (2007) 29.
[27] H.El. Kadiri, A.L. Oppedal, J. Mechs. Phys. Solids 58 (2010) 613.
[28] R.W. Armstrong, G.T.J. Horne, Iron. Steel Inst. 91 (1962) 311.
[29] R.W. Armstrong, F.J. Zerilli, Advances in Twinning, The Minerals Metals and Materials Society, 1999, pp. 67.
[30] T.N. Williams, R. Carino, Image Analyzer–A Software Tool for Calculating Certain Material Model Constants from Optical Images, MSU.CAVS.CMD.2007-R0039, 2007.